GeoAI for Disaster Mitigation: Fire Severity Prediction Models using Sentinel-2 and ANN Regression

by Syam'ani Syam'ani

GeoAI for Disaster Mitigation: Fire Severity Prediction Models using Sentinel-2 and ANN Regression

1st Syamani D. Ali
Center for Geospatial Information Infrastructure Development (PPIIG)
University of Lambung Mangkurat
Banjarbaru, Indonesia
syamani.fhut@ulm.ac.id

2nd Ichsan Ridwan
Center for Geospatial Information Infrastructure Development (PPIIG)
University of Lambung Mangkurat
Banjarbaru, Indonesia
ichsanridwan@ulm.ac.id

3rd Meldia Septiana
Center for Geospatial Information Infrastructure Development (PPIIG)
University of Lambung Mangkurat
Banjarbaru, Indonesia
meldia.septiana@ulm.ac.id

4th Abdi Fithria
Center for Geospatial Information Infrastructure Development (PPIIG)
University of Lambung Mangkurat
Banjarbaru, Indonesia
mksfabdi@ulm.ac.id

5th Arfa Agustina Rezekiah
Center for Geospatial Information Infrastructure Development (PPIIG)
University of Lambung Mangkurat
Banjarbaru, Indonesia
aarezekiah@ulm.ac.id

6th Adi Rahmadi
Center for Geospatial Information Infrastructure Development (PPIIG)
University of Lambung Mangkurat
Banjarbaru, Indonesia
arahmadi@ulm.ac.id

7th Mufidah Asyari
Center for Geospatial Information Infrastructure Development (PPIIG)
University of Lambung Mangkurat
Banjarbaru, Indonesia
mufie.ikhsan@ulm.ac.id

8th Hidayatul Rahman
Infrastructure and Territorial Section
Regional Development Planning
Agency of South Kalimantan Province
Banjarbaru, Indonesia
hidayatul.rahman0097@gmail.com

9th Gita Ayu Syafarina
Infrastructure and Territorial Section
Regional Development Planning
Agency of South Kalimantan Province
Banjarbaru, Indonesia
gitaayusyafarina@gmail.com

Abstract— Wildfire is a common disaster that hits Indonesia every dry season, especially on the islands of Kalimantan and Sumatra. In order to reduce the impact of fire hazards, preventive measures are needed before the occurrence of fires. One of them is by setting up an information system such as EWS. The aim of this study is to create an effective image- and machine learning-based predictive model of the severity of forest and land fires based on vegetation conditions prior to burning. Three parameters of prefire vegetation conditions, namely vegetation greenness indices, vegetation moisture, and vegetation senescence, were selected as independent variables to predict the postfire dependent variable, i.e., fire severity. There are 25 vegetation greenness index options tested, using either ANN regression or multiple linear regression. The vegetation moisture information is represented by the Normalized Difference Moisture Index (NDMI). The vegetation senescence information is extracted using the Plant Senescence Reflectance Index (PSRI). Meanwhile, the wildfire severity is measured using the Burned Area Index for Sentinel-2 (BAIS2). All vegetation conditions and wildfire severity information were extracted from Sentinel-2 imageries. The topology of ANN regression models is configured from one to six hidden layers. More than 100,000 pixels are used as samples, which are then separated into training samples and validation samples. The results of model development and testing show that ANN regression with Inverted Red-Edge Chlorophyll Index (IRECI) as a vegetation greenness parameter is the model that has the highest accuracy in predicting wildfire severity.

Keywords—fire disaster, Sentinel-2, machine learning, deep learning, artificial intelligence, artificial neural network

I. INTRODUCTION

Wildfire is one of the hazards that is included in the list of the top ten causes of disasters [16]. Of the total disasters that hit the world during 2000 to 2019, wildfire took the seventh position, which is 3% of all disasters that occurred during those 20 years [16]. In Indonesia, especially the islands of Kalimantan and Sumatra, forest and land fires are local disasters that have regional or even global impacts. Smoke from the forest and land fires can spread to neighboring countries and cause flight disruptions and various human health problems. Carbon emissions resulting from the forest and land fires will have a contribution to global warming.

Remote sensing technology can provide information on the earth's surface at the time before burning, during burning, or after burning. Before burning, remote sensing imagery can provide information on the availability and distribution of fuels. In the event of fires, remote sensing imagery can provide information on hotspots or active fires. And at the time after burning, remote sensing imagery can provide information on the burned area. As a remote sensing satellite, Sentinel-2 satellite imageries are freely available to public worldwide with moderate spatial accuracy and high spectral accuracy [55][26]. Sentinel-2 imagery offers a mapping method that is fast, inexpensive and easy to implement [46][20]. The thematic maps produced can provide more up-to-date information, because the availability of images can be obtained every 5 days [55][26][20][54]. In addition, Sentinel-2 imagery is available online directly on the day of its acquisition, making it effective for monitoring wildfire events or wildfire severity in near real-time.

Wildfire severity was defined as the degree of change in the soil and vegetation caused by fires. Fire severity indices are used to assess the impact of fire and burnt area extent. Fire severity mapping is crucial for the forest departments to set up mitigation measures and to restore the affected areas after the fire season [40] [53]. The severity of a fire is one of the factors controlling post-fire vegetation recovery and species composition [33]. In wildfire research, the terms burn severity and fire severity are often used interchangeably. Fire severity quantifies the immediate short-term fire effects on the local environment, whereas burn severity quantifies both the short and long-term impact as it includes response processes such as vegetation recovery [58][44].

Numerous severity indices have been developed, highlighting the standardized Normalized Burn Ratio (NBR), difference (dNBR), the standardized difference of NDVI (dNDVI), the relative version of dNBR (RdNBR), and Burned Area Index for Sentinel-2 (BAIS2) [40][53][13][56]; all of them used as independent variables used to deduce the field indices of severity at the pixel level. The Normalized Burn Ratio (NBR) is generally accepted as the standard spectral index for assessing fire severity. In case of heterogeneous landscapes, mapping of burn severity using Relativized dNBR is more suitable [31]. and some authors have highlighted the need for independent validation of the approach for specific regions and vegetation types [11].

The fuel for wild fires is almost entirely vegetation. While the distribution of vegetation features is very easy to identify on satellite imagery such as Sentinel-2. In remote sensing. In addition, there are also transformation methods to detect vegetation moisture, vegetation dryness, and so on. Where these parameters are strongly related to wildfire susceptibility. Therefore, by identifying the quantity, moisture, and dryness of the vegetation before it burns, we will basically be able to predict how severe the wildfire will be. In a nutshell, if we hypothesize that there is a correlation between the quantity and quality of vegetation features before burning with the wildfire severity levels that will occur, then we can simply build regression models to predict wildfire severity.

If we assume that the correlation between vegetation quantity/quality and wildfire severity is linear, then we can use linear regression. However, if the correlation is not linear, then we can use Artificial Neural Network (ANN) regression. Linear and ANN regression are machine learning algorithms. Meanwhile, machine learning itself is a subset of artificial intelligence (AI) technologies. If applied to geospatial information, then AI is often referred to as Geospatial Artificial Intelligence (GeoAI). GeoAI has its origins from GIScience methods applied to remote sensing data in order to tackle geospatial-specific big data challenges and problems [45]. GeoAI combines methods in spatial science, data mining, and high-performance computing to extract information from geospatial big data [49]. Nowadays, GeoAI applied in specific topic, such as spatially explicit model generation, question answering and summarization, social sensing and semantic signatures, even the moonshots [42].

There have been several previous studies using ANN to study wildfires. Whether it's for fire prediction [15][36][38][41][62], fire risk assessment [60], fire danger [47], fire susceptibility [28][43], fire scale [29], and so on. The purpose of this research is to develop an efficient image- and machine learning-based predictive model of the severity of forest and land fires that will occur based on vegetation conditions before burning. The main reasons for prioritizing the application of ANN regression over deciding to apply linear regression are the unknown distribution pattern of the data, and the unknown correlation trend between the quantity and quality of vegetation before burning and the severity of the wildfires that will occur. Given that ANN is a non-parametric method, whereas linear regression is a parametric method that has pre-assumptions before prediction. The model generated from this research is expected to be used to predict the possible severity of wildfires in the short term, such as in the next few days or weeks. Furthermore, the model will also be able to be used in the development of the fire Early Warning System (EWS).

II. RESEARCH METHODS

A. Study Area

This research was conducted in parts of South Kalimantan Province and parts of Central Kalimantan Province, Kalimantan Island, Indonesia. More precisely, the training area and testing area for sampling in the construction and validation of the regression model were carried out on three tiles of Sentinel-2 MSI imageries, namely T50MKA, T50MKB, and T50MKC, as shown in Fig. 1.
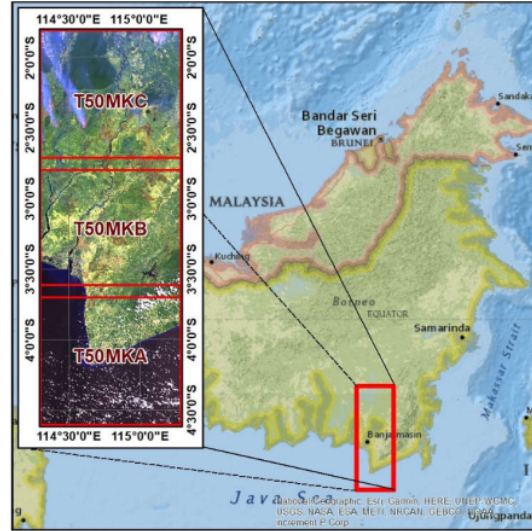

Fig. 1. Study area

B. Sentinel-2 Imagery

In the burned area and fire severity mapping, at least multitemporal images are required at two different times, i.e., prefire and postfire. In this study, the prefire imagery is the Sentinel-2 imagery, which was acquired on August 9, 2019, and the prefire imagery is the Sentinel-2 imagery, which was acquired on September 13, 2019. In addition, this study also provides Sentinel-2 imagery for the acquisition of October 23, 2019. The image for this October's acquisition is only used as a visual comparison of the results of model implementation.

C. Vegetation Indices

1) Vegetation Greenness: Vegetation greenness has a correlation with the quantity of vegetation. The higher the vegetation greenness value, the greater the quantity of vegetation, and, of course, the greater the volume of available fuel will be. There are lots of vegetation greenness indices that have been developed. However, only 25 of them will be tested in this research. More details can be seen in TABLE I.

2) Vegetation Moisture: The vegetation moisture describes the quality of the fuel. The lower the humidity level of the vegetation, the more susceptible it is to burn later. The parameter to measure vegetation moisture used in this research is the Normalized Difference Moisture Index (NDMI) [10], which is formulated as in (1).

$$NDMI = \frac{NIR - SWIR1}{NIR + SWIR1} \qquad (1)$$

Where:
SWIR1: Shortwave Infrared 1 band

3) Vegetation Senescence: Similar to vegetation moisture, vegetation senescence is also describe the fule quality. Vegetation senescence is basically used to identify vegetation that is mature or old. The higher the vegetation senescence value, the more vulnerable the vegetation is to burning. The parameter used to measure vegetation senescence in this study is the Plant Senescence Reflectance Index (PSRI) [50], which is formulated as in (2).

$$PSRI = \frac{Red - Blue}{RE2} \qquad (2)$$

PSRI is also used as masking in the model implementation for fire severity prediction. The vegetation that has a positive PSRI value or more than zero is considered to be burned later, while the rest will not burn.

D. Fire Severity Mapping

The model construction in this investigation is that the prefire vegetation conditions, i.e., vegetation greenness, vegetation moisture, and vegetation senescence, will determine the postfire fire severity. Of course, in this case, the fire severity is extracted from the burned area. The burned area identification was carried out using the Burned Area Index for Sentinel-2 (BAIS2) [23], which was formulated as in (3).

$$BAIS2 = \left(1 - \sqrt{\frac{RE2*RE3*NNIR}{Red}}\right) * \left(\frac{SWIR2-NNIR}{\sqrt{SWIR2+NNIR}} + 1\right) \qquad (3)$$

Where:
NNIR: Narrow Near Infrared band
SWIR2: Shortwave Infrared 2 band

TABLE I.   VEGETATION GREENNESS INDICES

No.	Vegetation Indices	Formula	Literatures
1	Soil Adjusted Vegetation Index (SAVI)	$SAVI = \frac{NIR-Red}{NIR+Red+L} x(1+L)$; Where: L = 0.5	[7]
2	Normalized Difference Vegetation Index (NDVI)	$NDVI = \frac{NIR-Red}{NIR+Red}$	[39]
3	Transformed Soil Adjusted Vegetation Index (TSAVI)	$TSAVI = \frac{s*(NIR-s*Red-a)}{s*NIR+Red-a*s+X*(1+s^2)}$ Where: a = 0.5, s = 0.5, X = 0.08	[21]
4	Modified Soil Adjusted Vegetation Index (MSAVI)	$MSAVI = \frac{(1+L)*(NIR-Red)}{NIR+Red+L}$ Where: $L = 1 - 2*s*NDVI*WDVI$; s = 0.5	[37]
5	Difference Vegetation Index (DVI)	$DVI = NIR - Red$	[6]
6	Ratio Vegetation Index (RVI)	$RVI = NIR/Red$	[19]
7	Perpendicular Vegetation Index (PVI)	$PVI = \frac{NIR-Red}{0.5*\sqrt{NIR+Red}}$	[6]
8	Infrared Percentage Vegetation Index (IPVI)	$IPVI = \frac{NIR}{NIR+Red}$	[57]
9	Weighted Difference Vegetation Index (WDVI)	$WDVI = NIR - a*Red$; Where: a = 0.460	[34]
10	Transformed Normalized Difference Vegetation Index (TNDVI)	$TNDVI = \sqrt{\frac{NIR-Red}{NIR+Red} + 0.5}$	[27]
11	Green Normalized Difference Vegetation Index (GNDVI)	$GNDVI = \frac{NIR-Green}{NIR+Green}$	[1]
12	Global Environmental Monitoring Index (GEMI)	$GEMI = \eta*(1-0.25*\eta) - \frac{Red-0.125}{1-Red}$ Where: $\eta = \frac{2*(NIR^2-Red^2)+1.5*NIR+0.5*Red}{NIR+Red+0.5}$	[12]
13	Atmospherically Resistant Vegetation Index (ARVI)	$ARVI = \frac{NIR-(2*Red-Blue)}{NIR+(2*Red-Blue)}$	[61]
14	Normalized Difference Index 45 (NDI45)	$NDI45 = \frac{RE1-Red}{RE1+Red}$	[32]
15	Modified Chlorophyll Absorption Reflectance Index (MCARI)	$MCARI = \left((RE1-Red)-0.2*(RE1-Green)\right)*\frac{RE1}{Red}$	[17]
16	Enhanced Vegetation Index (EVI)	$EVI = 2,5*\frac{NIR-Red}{NIR+6Red-7,5Blue+1}$	[5]
17	Sentinel-2 Red-Edge Position Index (S2REP)	$S2REP = 705+35*\frac{(Red+RE3)/2-RE1}{RE2-RE1}$	[25]
18	Inverted Red-Edge Chlorophyll Index (IRECI)	$IRECI = \frac{RE3-Red}{RE1/RE2}$	[35]
19	Pigment Specific Simple Ratio (PSSRa)	$PSSRa = RE3/Red$	[24]
20	Anthocyanin Reflectance Index (ARI)	$ARI = 1/Green - 1/RE1$	[3]
21	Green Leaf Index (GLI)	$GLI = \frac{2*Green-Red-Blue}{2*Green+Red+Blue}$	[52]
22	Leaf Chlorophyll. Index (LCI)	$LCI = \frac{NIR-RE1}{NIR-Red}$	[8][9]
23	Chlorophyll Vegetation Index (CVI)	$CVI = \frac{NIR*Red}{Green^2}$	[52]
24	Carotenoid Reflectance Index 550 nm (CRI550)	$CRI550 = 1/Blue - 1/Green$	[2]
25	Carotenoid Reflectance Index 700 nm (CRI700)	$CRI700 = 1/Blue - 1/RE1$	[51]

a. NIR: Near Infrared band; RE1: Red Edge 1 band; RE2: Red Edge 2 band; RE3: Red Edge 3 band

Henceforth, the classification of the fire severity in the burned area is carried out on the change in BAIS2 values between postfire and prefire, as formulated in (4). Equation (4) is a modification of [23], it aims to be able to use the United States Geological Survey (USGS) fire severity criteria later.

$$dBAIS2 = BAIS2_{postfire} - BAIS2_{prefire} \qquad (4)$$

TABLE II.   FIRE SEVERITY CLASSIFICATION BASED ON DBAIS2

Severity Level	dBAIS2 Range
Unburned	< 0.100
Low Severity	0.100 - < 0.270
Moderate-low Severity	0.270 - < 0.440
Moderate-high Severity	0.440 - < 0.660
High Severity	> 0.660

The determination of the severity of the fire itself refers to the USGS criteria [14][18] as shown in TABLE II. This criterion was also slightly modified in value, including the elimination of the vegetation growth after burning.

E. Artificial Neural Network Regression

Let y be the dependent variable; x_1, x_2, x_3, to x_n are independent variables with the respective coefficients being ω_1, ω_2, ω_3, to ω_n, while b is the intercept. The relationship can be notated into multiple linear regression [48] as in (5).

$$y = \omega_1 x_1 + \omega_2 x_2 + \omega_3 x_3 + \cdots + \omega_n x_n + b \qquad (5)$$

For simplicity, the linear regression equation in (5) can also be denoted into vector equation as in (6).

$$y = \omega^T x + b \qquad (6)$$

Henceforward, if W_1, W_2, W_3, to W_n, each is a hidden layer with n nodes, B_1, B_2, B_3, each is a bias, and α is the activation function, then the Artificial Neural Network (ANN) [59] regression with three hidden layers is formulated as in (7).

$$y = W_3^T \alpha\left(W_2^T \alpha\left(W_1^T \alpha\left(\omega^T x + b\right) + B_1\right) + B_2\right) + B_3 \qquad (7)$$

Where the activation function α is the Rectified Linear Unit (ReLU) [4] which is formulated as in (8).

$$\alpha = \begin{cases} x, & x > 0 \\ 0, & x \leq 0 \end{cases} \qquad (8)$$

The linear and ANN regression is implemented using the Python and Scikit-Learn [22]. For practical purposes, the outputs of regression models are all stored in files (.sav files), and later when executed on a Sentinel-2 imagery, these model files must also be called and run using Python and Scikit-Learn. All developed program codes, including output from regression models, are stored at the Github repository https://github.com/syamaniulm/ann-fire-severity.

F. Water Index

Some vegetation indices, are very sensitive to water, especially turbid water. As a result, the turbid water has the potential to be identified as a burned area. Thus, the body of water needs to be masked. The method used for masking water bodies is the Modified Normalized Difference Water Index (MNDWI) [30], as formulated in (9).

$$MNDWI = \frac{Green - SWIR1}{Green + SWIR1} \qquad (9)$$

G. Model Training and Validation

Linear and ANN regression are supervised machine learning techniques, so they require training. In this context, the training areas in question are burned areas. There are more than 100,000 pixel burned areas that are used as training areas in this study. These training areas are separated into two clusters, i.e., 80% for the training data and the remaining 20% for the validation data. The capability of each model was assessed using three parameters, namely correlation coefficient (R^2), Mean Absolute Percentage Error (MAPE), and Root Mean Square Error (RMSE). The best model is assessed by the highest R^2 value (closest to 1) and the lowest MAPE and RMSE values (closest to 0). The whole process of computing R^2, MAPE, and RMSE is done automatically using Python. R^2 is calculated using training data, while MAPE and RMSE are calculated using validation data.

III. RESULTS AND DISCUSSION

The ANN used in this research is Multilayer Perceptron (MLP). In addition to the number of hidden layers, the number of nodes for each layer, and the activation function that is set in such a way, other parameters such as alpha, solver, learning rate, and so on, are left in their default settings. Especially for setting the number of hidden layers, in this research it is limited to six hidden layers. In Fig. 2, it can be seen that for ANN regression there are three models with the highest R^2 and accuracy, namely SAVI, WDVI, and IRECI. And each of the three is an ANN regression with six hidden layers. Of these three vegetation indices, ANN with IRECI as the vegetation greenness parameter is the best model. This can be seen from the highest R^2 value and the lowest MAPE and RMSE values. The R^2 value of this model is 0.9154, and the MAPE value is 9.52%. Because it has the highest correlation and accuracy, for practical purposes later on, we will recommend this model.

Compared to ANN, linear regression has a simpler model. However, linear regression has several conditions to be accepted statistically. Among these conditions is that there is a linear relationship between the dependent and independent variables. And in the real world, this is often not the case. As seen in Fig. 3, it can be seen that all of the multiple linear regression models applied in this research as a comparison for ANN regression, none of them have any accuracy that can outperform ANN regression. This shows that the relationship between fire severity and the three independent variables in this research tends to have non-linear patterns. Thus, the application of ANN regression is generally more optimal.

As an implementation example, we apply IRECI and MCARI. Since IRECI is the best model for ANN regression and MCARI is the best model for linear regression. The result is as shown in Fig. 4. In Fig. 4, we also present real fire severity facts based on Sentinel-2 imageries acquired on September 13, 2019 and October 23, 2019. If we visually compare the predictions, using both ANN and linear regression, to the fact of fire severity, it looks as if the prediction results have a fairly large commission error. Practically speaking, this cannot be translated as an error. Given that this research is not in order to identify where fires will burn. Rather, this research is only to predict if fires occur in certain locations, then how severe the fires will be. Of course, in the real world, areas that have the potential to be severely burned may not experience fires due to many factors. Such as the absence of sources of fire, including the mitigation actions taken by humans.

Fig. 2.   Artificial neural network regression analysis results

	R2 (1H)	MAPE (1H)	RMSE (1H)	R2 (2H)	MAPE (2H)	RMSE (2H)	R2 (3H)	MAPE (3H)	RMSE (3H)	R2 (4H)	MAPE (4H)	RMSE (4H)	R2 (5H)	MAPE (5H)	RMSE (5H)	R2 (6H)	MAPE (6H)	RMSE (6H)
SAVI	0.8956	10.49	0.6984	0.9051	10.07	0.6654	0.9108	10.02	0.6460	0.9083	9.73	0.6556	0.9163	9.65	0.6275	0.9135	9.80	0.6381
NDVI	0.8339	13.65	0.8708	0.8413	12.93	0.8504	0.8497	12.83	0.8247	0.8532	12.57	0.8178	0.8445	13.04	0.8375	0.8592	12.44	0.7995
TSAVI	0.8905	11.08	0.7101	0.9028	10.72	0.6708	0.8987	11.19	0.6849	0.9072	9.99	0.6571	0.9060	9.88	0.6626	0.9087	9.97	0.6528
MSAVI	0.8976	10.33	0.6916	0.9044	10.19	0.6665	0.9095	10.21	0.6508	0.9092	9.61	0.6532	0.9048	10.23	0.6652	0.9094	10.07	0.6523
DVI	0.8861	10.79	0.7293	0.8931	10.74	0.7057	0.9046	9.83	0.6709	0.9055	9.70	0.6663	0.9070	9.79	0.6610	0.9017	9.79	0.6817
RVI	0.8410	13.43	0.8485	0.8327	13.24	0.8725	0.8437	13.53	0.8418	0.8456	13.25	0.8361	0.8413	13.84	0.8492	0.8363	13.70	0.8603
PVI	0.8846	11.56	0.7323	0.8944	10.54	0.7021	0.9024	10.22	0.6774	0.9012	9.84	0.6830	0.9080	9.73	0.6582	0.9003	9.79	0.6870
IPVI	0.8226	13.87	0.8995	0.8408	13.23	0.8511	0.8480	13.02	0.8296	0.8549	12.85	0.8114	0.8542	12.67	0.8129	0.8480	12.72	0.8338
WDVI	0.8900	10.98	0.7160	0.8995	10.87	0.6847	0.9085	10.12	0.6548	0.9037	10.03	0.6724	0.9068	10.09	0.6585	0.9123	9.90	0.6428
TNDVI	0.8176	14.14	0.9125	0.8274	14.03	0.8859	0.8463	13.25	0.8509	0.8563	12.95	0.8240	0.8563	12.93	0.8068	0.8558	12.58	0.8079
GNDVI	0.8085	14.45	0.9343	0.8251	13.92	0.8910	0.8319	13.30	0.8762	0.8439	12.70	0.8497	0.8453	13.17	0.8420	0.8407	12.71	0.8562
GEMI	0.8784	10.95	0.7539	0.8962	10.40	0.6982	0.8997	10.39	0.6871	0.8995	9.93	0.6876	0.9022	10.26	0.6780	0.8959	10.03	0.7014
ARVI	0.8307	13.79	0.8789	0.8404	12.97	0.8528	0.8465	13.01	0.8337	0.8520	12.94	0.8196	0.8467	12.87	0.8326	0.8564	12.71	0.8081
NDI45	0.8660	11.89	0.7801	0.8690	11.92	0.7707	0.8761	11.46	0.7511	0.8756	11.31	0.7536	0.8792	11.44	0.7419	0.8763	11.48	0.7520
MCARI	0.9003	10.08	0.6776	0.9023	10.14	0.6701	0.9060	9.66	0.6578	0.9088	9.68	0.6503	0.9044	10.13	0.6656	0.9045	9.92	0.6660
EVI	0.8840	11.11	0.7357	0.8911	10.76	0.7127	0.9007	10.21	0.6826	0.9005	9.92	0.6833	0.9044	9.94	0.6710	0.9019	10.29	0.6780
S2REP	-4.6961	104.94	5.1206	-2.7771	85.23	4.1682	0.3848	26.22	1.6887	0.7823	15.98	0.9965	0.7929	15.29	0.9738	0.7829	15.94	0.9944
IRECI	0.8930	10.60	0.7030	0.9045	10.05	0.6656	0.9102	9.75	0.6435	0.9049	10.40	0.6618	0.9096	9.53	0.6496	0.9154	9.52	0.6279
PSSRa	0.8524	13.00	0.8184	0.8413	12.84	0.8523	0.8555	12.59	0.8118	0.8571	12.48	0.8087	0.8615	12.35	0.7932	0.8556	13.03	0.8119
ARI	0.8060	14.46	0.9425	0.7976	14.18	0.9636	0.8054	14.17	0.9427	0.8162	13.93	0.9178	0.8166	14.04	0.9153	0.8140	14.20	0.9239
GLI	0.8496	13.32	0.8316	0.8517	12.46	0.8271	0.8620	12.20	0.7978	0.8629	12.67	0.7935	0.8647	12.41	0.7888	0.8659	12.30	0.7853
LCI	0.8096	14.46	0.9333	0.8288	13.22	0.8880	0.8362	13.04	0.8660	0.8416	13.10	0.8545	0.8431	12.94	0.8487	0.8406	12.59	0.8590
CVI	0.8016	14.63	0.9516	0.8051	14.26	0.9443	0.8136	13.76	0.9243	0.8214	14.12	0.9071	0.8317	13.44	0.8840	0.8193	13.98	0.9112
CRI550	0.8194	14.14	0.9092	0.8351	13.38	0.8661	0.8361	13.27	0.8632	0.8358	12.93	0.8662	0.8395	12.69	0.8548	0.8437	12.86	0.8442
CRI700	0.8185	14.30	0.9081	0.8149	14.42	0.9149	0.8222	14.16	0.8999	0.8322	13.57	0.8714	0.8397	13.33	0.8528	0.8214	13.54	0.9065

Although ANN regression has the best ability to predict wildfire severity, this model is relatively difficult to implement for practical purposes. Apart from execution time issues, ANN regression must be implemented using a programming language such as Python. Henceforward, the application of ANN regression requires operators or analysts to understand programming languages. Especially for the execution time problem, in this research we try to provide a solution by developing optimized Python codes to be executed on every Sentinel-2 imagery tile. Furthermore, if hardware resources are very limited, in later processing the image can be reduced in dimensions. As long as the dimensions of the rows and columns of the image are identical, for example, 1,000 x 1,000 pixels. Users who have quite a bit of programming skills can, of course, take advantage of the source code of the program that we have prepared in our repository, as mentioned in section II.E, complete with the instructions for use. Meanwhile, users who are already proficient in programming, especially Python, can of course modify or optimize the source code that we have written.

The models developed in this research are limited to how to predict the fire severity that will occur based on the quantity and quality of fuel. In short, this research only develops models to provide one of the input parameters in the geospatial EWS. Therefore, for the purposes of developing wildfire EWS, it is necessary to add other geospatial parameters. Such as air temperature, wind speed, wind direction, real-time existing hotspots, and even human accessibility information, such as roads. Furthermore, because the models developed in this research are short-term wildfire severity prediction models, it is recommended that information on vegetation conditions be updated regularly in the EWS. For example, every five days, referring to the temporal resolution of Sentinel-2 satellites.

|	Intercept	VI Coef.	NDMI Coef.	PSRI Coef.	R2	MAPE	RMSE
SAVI	-0.1083	1.8531	0.2658	0.5148	0.8751	12.36	0.7633
NDVI	0.0355	0.7245	0.9428	0.9269	0.7973	15.60	0.9630
TSAVI	-0.1369	1.6884	0.3927	0.9876	0.8536	13.14	0.8218
MSAVI	0.0413	1.5907	0.2697	0.3102	0.8808	12.19	0.7454
DVI	0.1317	2.3590	0.3528	0.0689	0.8738	12.22	0.7684
RVI	0.3599	0.0372	0.8595	0.3230	0.8211	14.45	0.8998
PVI	0.1317	3.3362	0.3528	0.0689	0.8738	12.22	0.7684
IPVI	-0.6889	1.4489	0.9428	0.9269	0.7973	15.60	0.9630
WDVI	0.1722	2.2165	0.4598	0.5601	0.8612	13.10	0.8039
TNDVI	-0.8381	1.2552	1.0176	0.8684	0.7911	15.95	0.9783
GNDVI	0.3409	0.3352	1.1828	0.3085	0.7810	16.49	1.0009
GEMI	-0.2745	1.4179	0.4279	0.0438	0.8642	12.46	0.7968
ARVI	-0.0002	0.8260	0.8788	1.4288	0.8012	15.26	0.9527
NDI45	0.0383	1.3550	0.6857	0.9099	0.8540	12.63	0.8131
MCARI	0.3191	2.3848	0.6021	0.2488	0.8839	11.44	0.7312
EVI	-0.0241	1.5352	0.3509	0.5490	0.8714	12.33	0.7720
S2REP	5.2430	-0.0065	1.2805	0.0900	0.7829	16.17	0.9986
IRECI	0.3265	0.6374	0.5690	0.1881	0.8545	13.16	0.8193
PSSRa	0.3447	0.0414	0.8351	0.3490	0.8307	14.10	0.8751
ARI	0.5760	-0.0033	1.2604	0.1102	0.7766	16.47	1.0122
GLI	0.3646	1.0461	0.7399	0.4916	0.8283	14.11	0.8887
LCI	0.5114	0.0855	1.2443	0.2130	0.7758	16.60	1.0133
CVI	0.5711	-0.0073	1.2745	0.1689	0.7762	16.55	1.0127
CRI550	0.5028	0.0041	1.1179	0.1426	0.7928	15.89	0.9725
CRI700	0.4964	0.0026	1.1818	0.1875	0.7858	16.27	0.9890

Fig. 3.   Linear regression analysis results
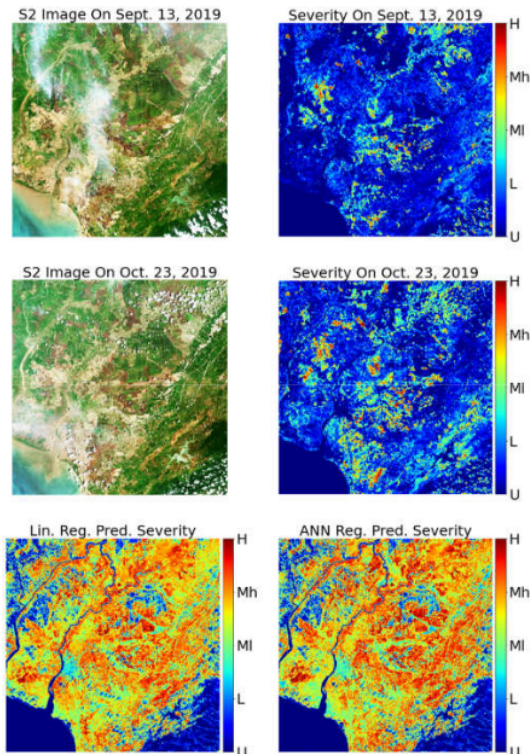
Fig. 4. Sentinel-2 true color composite image, actual existing fire severity, and fire severity prediction results (H: High Severity; Mh: Moderate-high Severity; Ml: Moderate-low Severity; L: Low Severity; U: Unburned)

IV. CONCLUSIONS

In general, ANN regression is able to produce very accurate wildfire severity predictions, even more than 90% accuracy. In a practical sense, this accuracy is very capable and can be accounted for. However, ANN regression has limitations in terms of implementation efficiency. ANN requires programming skills for the analyst who will execute the model. Among all the vegetation greenness indices tested, especially for ANN regression, three vegetation greenness indices, i.e., SAVI, WDVI, and IRECI, are the best. In the implementation, you can choose one of the three, or directly choose the highest of the three, namely IRECI. Besides being the most accurate, the IRECI mathematical transformation model is also very simple. For the analysts who lack knowledge of programming languages, of course, they can take advantage of the multiple linear regression model using MCARI. Of course, with the consequence of losing accuracy compared to the ANN regression model.

REFERENCES

[1] A.A. Gitelson, Y.J. Kaufman, and M.N. Merzlyak, "Use of a green channel in remote sensing of global vegetation from EOS-MODIS," Remote Sens. Environ., 58, 1996, pp. 289-298.

[2] AA. Gitelson, M.N. Merzlyak, and O.B. Chivkunova, "Optical properties and nondestructive estimation of anthocyanin content in plant leaves," Photochem. Photobiol., 74, 2001, pp. 38-45.

[3] A.A. Gitelson, O.B. Chivkunova, and M.N. Merzlyak, "Nondestructive estimation of anthocyanins and chlorophylls in anthocyanic leaves," Am. J. Bot., 96, 2009, pp. 1861-1868.

[4] A.F. Agarap, "Deep Learning using Rectified Linear Units (ReLU)" arXiv preprint arXiv:180308375, 2018.

[5] A. Huete, K. Didan, T. Miura, E.P. Rodriguez, X. Gao, and L.G. Ferreira, "Overview of the radiometric and biophysical performance of the MODIS vegetation indices," Remote Sens. Environ., 83, 2002, pp. 195-213.

[6] A.J. Richardson and C. Weigand, "Distinguishing Vegetation from Soil Background Information," Photogrammetric Engineering and Remote Sensing, 43 (12), 1977, pp. . 1541-1552.

[7] A.R. Huete, "A soil-adjusted vegetation index (SAVI)," Remote Sens. Environ., 25, 1988, pp. 295–309.

[8] B .Datt, "A new reflectance index for remote sensing of chlorophyll content in higher plants: tests using Eucalyptus leaves," J. Plant Physiol., 154, 1999a, pp. 30-36.

[9] B. Datt, "Remote sensing of water content in Eucalyptus leaves," Aust. J. Bot., 47, 1999b, pp. 909-923.

[10] B. Gao, "NDWI—A normalized difference water index for remote sensing of vegetation liquid water from space," Remote Sens. Environ., 58 (3), 1996, pp. 257-266.

[11] B. N. Tran, M. A. Tanase, L. T. Bennett, and C. Aponte, "Evaluation of spectral indices for assessing fire severity in Australian temperate forests," Remote Sens., 10 (11), 2018, pp. 1-18.

[12] B. Pinty and M. M. Verstraete, "GEMI: a non-linear index to monitor global vegetation from satellites," Vegetatio, 101, 1992, pp. 15-20.

[13] C. Fernández, J. M. Fernández-Alonso, J. A. Vega, T. Fontúrbel, R. Llorens, and J. A. Sobrino, "Exploring the use of spectral indices to assess alterations in soil properties in pine stands affected by crown fire in Spain," Fire Ecol., 17 (2), 2021.

[14] C.H. Key and N.C. Benson, "Measuring and remote sensing of burn severity," Joint Fire Science Conference and Workshop Proceedings, 2000, pp. 284-285.

[15] C. Lai, S. Zeng, W. Guo, X. Liu, Y. Li, and B. Liao, "Forest Fire Prediction with Imbalanced Data Using a Deep Neural Network Method," Forests, 13 (7), 2022, p. 1129.

[16] CRED and UNDRR, The Human Cost of Disasters - An overview of the last 20 years 2000-2019, Centre for Research on the Epidemiology of Disasters (CRED), Brussels, and United Nations Office for Disaster Risk Reduction (UNDRR), Geneva, 2020.

[17] C.S.T. Daughtry, C.L. Walthall, M.S. Kim, E. Brown de Colstoun, J.E. McMurtrey III, "Estimating Corn Leaf Chlorophyll Concentration from Leaf and Canopy Reflectance," Remote Sens. Environ., 74 (2), 2000, pp. 229-239.

[18] D.C. Lutes, R.E. Keane, J.F. Caratti, C.H. Key, N.C. Benson, S. Sutherland, and L.J. Gangi, "FIREMON: Fire Effects Monitoring and Inventory System," General Technical Report RMRS-GTR-164-CD, Fort Collins, CO, United States Department of Agriculture, Forest Service, Rocky Mountain Research Station, Retrieved from https://www.fs.usda.gov/rm/pubs_series/rmrs/gtr/rmrs_gtr164.pdf, 2006.

[19] D.J. Major, F. Baret, and G. Guyot, "A ratio vegetation index adjusted for soil brightness," Int. J. Remote Sens., 11, 1990, pp. 727-740.

[20] D. Notti, M. Cignetti, D. Godone, and D. Giordan, "Semi-automatic mapping of shallow landslides using free Sentinel-2 and Google Earth Engine," Nat. Hazards Earth Syst. Sci. Discuss. [preprint], https://doi.org/10.5194/nhess-2022-189, in review, 2022.

[21] F. Baret, and G. Guyot, "Potential and limits of vegetation indices for LA1 and APAR assessment," Remote Sens. Environ., 35, 1991, pp. 161-173.

[22] F. Pedregosa, G. Varoquaux, A. Gramfort, V. Michel, B. Thirion, O. Grisel, M. Blondel, P. Prettenhofer, R. Weiss, V. Dubourg, J. Vanderplas, A. Passos, D. Cournapeau, M. Brucher, M. Perrot, É.

Duchesnay, "Scikit-learn: Machine Learning in Python," Journal of Machine Learning Research, 12 (85), 2011, pp. 2825-2830.

[23] F. Filipponi, "BAIS2: Burned Area Index for Sentinel-2," Proceedings, 2 (7), 2018, p. 364.

[24] G.A. Blackburn, "Quantifying chlorophylls and carotenoids at leaf and canopy scales: an evaluation of some hyperspectral approaches," Remote Sens. Environ., 66, 1998, pp. 273-285.

[25] G. Guyot, and F. Baret, "Utilisation de la haute resolution spectrale pour suivre l'etat des couverts vegetaux," Proceedings 4th Int. Coll. Spectral Signatures of Objects in Remote Sensing, Aussois, France, ESA SP-287, 1988, pp. 279-286.

[26] G. Kuc and J. Chormański, "Sentinel-2 imagery for mapping and monitoring imperviousness in urban areas," Int. Arch. Photogramm. Remote Sens. Spat. Inf. Sci. - ISPRS Arch., 42 (1/W2), 2019, pp. 43-47.

[27] G.M. Senseman, C.F. Bagley, and S.A Tweddale, "Correlation of rangeland cover measures to satellite-imagery-derived vegetation indices," Geocarto International, 11 (3), 1996, pp. 29-38.

[28] G. Zhang, M. Wang, and K. Liu, "Deep neural networks for global wildfire susceptibility modelling," Ecological Indicators, 127, 2021, 107735.

[29] H. Liang, M. Zhang and H. Wang, "A Neural Network Model for Wildfire Scale Prediction Using Meteorological Factors," in IEEE Access, 7, 2019, pp. 176746-176755.

[30] H. Xu, "Modification of Normalized Difference Water Index (NDWI) to Enhance Open Water Features in Remotely Sensed Imagery," Int. J. Remote Sens., 27 (14), 2006, pp. 3025-3033.

[31] J.D. Miller and A. E. Thode, "Quantifying burn severity in a heterogeneous landscape with a relative version of the delta Normalized Burn Ratio (dNBR)," Remote Sens. Environ., 109 (1), 2007, pp. 66-80.

[32] J. Delegido, J. Verrelst, L. Alonso, and J. Moreno, "Evaluation of Sentinel-2 Red-Edge Bands for Empirical Estimation of Green LAI and Chlorophyll Content," Sensors, 11 (7), 2011, pp. 7063-7081.

[33] J. Epting and D. Verbyla, "Landscape-level interactions of prefire vegetation, burn severity, and postfire vegetation over a 16-year period in interior Alaska," Can. J. For. Res., 35 (6), 2005, pp. 1367-1377.

[34] J.G.P.W. Clevers, "Application of the WDVI in estimating LAI at the generative stage of barley," ISPRS J. Photogramm. Remote Sens., 46 (1), 1991, pp. 37-47.

[35] J.G.P.W. Clevers, S.M. De Jong, G.F. Epema, E.A. Addink, "MERIS and the Red-Edge Index," Second EARSeL Workshop on Imaging Spectroscopy, 2000, Enschede.

[36] J. Joshi and R. Sukumar, "Improving prediction and assessment of global fires using multilayer neural networks," Sci Rep, 11, 2021, p. 3295.

[37] J. Qi, A. Chehbouni, A.R. Huete, Y.H. Kerr, and Sorooshian, S., "A modified soil adjusted vegetation index," Remote Sens. Environ., 48 (2), 1994, pp. 119-126.

[38] J.R. Bergado, C. Persello, K. Reinke, and A. Stein, "Predicting wildfire burns from big geodata using deep learning," Safety Science, 140, 2021, 105276.

[39] J. W. Rouse, R. H. Haas, J. A. Schell, and D. W. Deering, "Monitoring vegetation systems in the Great Plains with ERTS," Third ERTS Symposium, NASA SP-351 I, 1973, pp. 309-317.

[40] K. D. Kovács, "Evaluation of Burned Areas With Sentinel-2 Using Snap: The Case of Kineta and Mati, Greece, July 2018," Tech. Geogr., 14 (2), 2019, pp. 20-38.

[41] K. Gao, Z. Feng, and S. Wang, "Using Multilayer Perceptron to Predict Forest Fires in Jiangxi Province, Southeast China," Discrete Dynamics in Nature and Society, Article ID 6930812, 2020.

[42] K. Janowicz, S. Gao, G. McKenzie, Y. Hu, and B. Bhaduri, "GeoAI: spatially explicit artificial intelligence techniques for geographic knowledge discovery and beyond," International Journal of Geographical Information Science, 34 (4), 2020, pp. 625-636.

[43] L.K. Sharma, R. Gupta, and N. Fatima, "Assessing the predictive efficacy of six machine learning algorithms for the susceptibility of Indian forests to fire," International Journal of Wildland Fire, 31, 2022, pp. 735-758.

[44] L. Schepers, B. Haest, S. Veraverbeke, T. Spanhove, J. Vanden Borre, and R. Goossens, "Burned area detection and burn severity assessment of a heathland fire in belgium using airborne imaging spectroscopy (APEX)," Remote Sens., 6 (3), 2014, pp. 1803-1826.

[45] L. Yang, J. Driscol, S. Sarigai, Q. Wu, H. Chen, and C. D. Lippitt, "Google Earth Engine and Artificial Intelligence (AI): A Comprehensive Review," Remote Sensing, 14 (14), 2022, p. 3253.

[46] L. Zhang, Q. Hu, and Z. Tang, "Using Sentinel-2 Imagery and Machine Learning Algorithms to Assess the Inundation Status of Nebraska Conservation Easements during 2018–2021," Remote Sensing, 14 (17), 2022, p. 4382.

[47] M. Bisquert, E. Caselles, J.M. Sánchez, and V. Caselles, "Application of artificial neural networks and logistic regression to the prediction of forest fire danger in Galicia using MODIS data," International Journal of Wildland Fire, 21, 2012, pp. 1025-1029.

[48] M. Krzywinski, N. Altman, "Multiple linear regression," Nature Methods, 12, 2015, pp. 1103-1104.

[49] M.N.K. Boulos, G. Peng, T. VoPham, "An overview of GeoAI applications in health and healthcare," International Journal of Health Geographics, 18 (7), 2019.

[50] M.N. Merzlyak, A.A. Gitelson, O.B. Chivkunova, and V.Y.U. Rakitin, "Non-destructive optical detection of pigment changes during leaf senescence and fruit ripening," Physiologia Plantarum, 106 (1), 1999, pp. 135-141.

[51] M.N. Merzlyak, A.A. Gitelson, O.B. Chivkunova, A.E. Solovchenko, S.I. Pogosyan, "Application of Reflectance Spectroscopy for Analysis of Higher Plant Pigments," Russ. J. Plant Physiol., 50, 2003, pp. 70-710.

[52] N. Gobron, B. Pinty, M.M. Verstraete, J.L. Widlowski, "Advanced vegetation indices optimized for up-coming sensors: design, performance, and applications," IEEE Trans. Geosci. Remote. Sens., 38, 2000, pp. 2489-2505.

[53] P. Konkathi and A. Shetty, "Assessment of Burn Severity using Different Fire Indices: A Case Study of Bandipur National Park," Proc. 2019 IEEE Recent Adv. Geosci. Remote Sens. Technol. Stand. Appl. TENGARSS 2019, 2019, pp. 151-154.

[54] P. Lemenkova, "Sentinel-2 for High Resolution Mapping of Slope-Based Vegetation Indices Using Machine Learning By SAGA GIS," Transylvanian Rev. Syst. Ecol. Res., 22 (3), 2020, pp. 17-34.

[55] Q. Wang and P. M. Atkinson, "Spatio-temporal fusion for daily Sentinel-2 images," Remote Sens. Environ., 204, 2018, pp. 31-42.

[56] R. Al-Hasn and R. Almuhammad, "Burned area determination using Sentinel-2 satellite images and the impact of fire on the availability of soil nutrients in Syria," J. For. Sci., 68 (3), 2022, pp. 96-106.

[57] R.E. Crippen, "Calculating the vegetation index faster," Remote Sens. Environ., 34, 1990, pp. 71-73.

[58] S. Veraverbeke, S. Lhermitte, W. W. Verstraeten, and R. Goossens, "The temporal dimension of differenced Normalized Burn Ratio (dNBR) fire/burn severity studies: The case of the large 2007 Peloponnese wildfires in Greece," Remote Sens. Environ., 114 (11), 2010, pp. 2548–2563.

[59] W.S. McCulloch and W. Pitts, "A logical calculus of the ideas immanent in nervous activity," The Bulletin of Mathematical Biophysics, 5 (4), 1943, pp. 115-133.

[60] Y. J. Goldarag, A. Mohammadzadeh, and A.S. Ardakani, "Fire Risk Assessment Using Neural Network and Logistic Regression," J Indian Soc Remote Sens., 44, 2016, pp. 885-894.

[61] Y.J. Kaufman, and D. Tanre, "Atmospherically resistant vegetation index (ARVI) for EOS-MODIS," IEEE Trans. Geosci. Remote Sens., 30, 1992, pp. 261-270.

[62] Y. Li, Z. Feng, S. Chen, Z. Shao, and F. Wang, "Application of the Artificial Neural Network and Support Vector Machines in Forest Fire Prediction in the Guangxi Autonomous Region, China," Discrete Dynamics in Nature and Society, Article ID 5612650, 2020.

GeoAI for Disaster Mitigation: Fire Severity Prediction Models using Sentinel-2 and ANN Regression